JOURNAL OF MATERIALS SCIENCE 29 (1994) 2481–2486

Toughened-hybrid epoxies: influence of the rubber-phase morphology on mechanical properties

C. I. VALLO, LIJIANG HU*, P. M. FRONTINI, R. J. J. WILLIAMS‡
Institute of Materials Science and Technology (INTEMA), University of Mar del Plata and National Research Council (CONICET). J.B. Justo 4302, (7600) Mar del Plata, Argentina

A toughened-epoxy polymer based on diglycidylether of bisphenol A (DGEBA) cured with ethylenediamine (EDA) and modified with a rubber based on an epoxy-terminated acrylonitrile–butadiene random copolymer (ETBN), exhibited different morphologies depending on the rubber content. Up to 10% rubber, the morphology consisted of a random dispersion of spherical domains rich in rubber, while at 15% rubber, large and irregular domains were present, turning into a co-continuous structure at 20% rubber. Mechanical properties (elastic modulus, uniaxial compression yield stress, critical stress intensity factor, K_{IC} and strain energy release rate, G_{IC}) of the toughened epoxies and hybrid-particulate materials containing glass beads, were analysed. The best mechanical properties were exhibited by hybrids with a random dispersion of rubbery domains in the epoxy matrix. The presence of large and irregular domains or co-continuous structures led to materials with poor mechanical properties.

1. Introduction

Unmodified epoxies are brittle polymers with poor resistance to crack propagation. A considerable increase in the crack resistance is obtained by generating a particulate-dispersed second phase. Particles may be either rubbery in character (generated *in situ* during the polymerization or present as a fine dispersion in the initial formulation), or rigid, such as alumina, silica or glass beads.

The presence of a dispersion of rubbery particles, with sizes in the range 0.1–5 μm, produces an increase in fracture toughness at the expense of a decrease in other mechanical properties, such as the elastic modulus and the yield stress [1]. Rigid particles lead to an increase in fracture toughness and elastic modulus [2–7]. The compression yield stress shows a variable behaviour depending on the nature of the particles and the previous surface treatment. The usual behaviour is an increase in the yield stress with the volume fraction of rigid particles. Exceptions were found for dolomite particles where the yield stress was constant [4], and for glass beads, either untreated or treated with compounds reducing the interfacial adhesion, where the yield stress decreased with the filler fraction [5].

The use of both types of particles leads to hybrid–particulate composites with enhanced values of crack resistance [8]. Analysis of toughening mechanisms revealed that the rigid particles increase the crack resistance mainly through a crack-pinning mechanism, whilst the rubbery particles enhance the extent of localized plastic shear deformations around the crack tip [9–11]. Formulations containing a fixed rubber amount (15% by weight in the epoxy matrix), showed a maximum in the critical stress intensity factor, K_{IC}, at room temperature, when plotted as a function of the volume fraction of filler [10, 12, 13]. Debonding of particles at high volume fractions has been suggested as the origin of such a maximum [10]. Very high values of K_{IC} resulted from the use of alumina fibre in hybrid epoxies [14].

The effect of varying the rubber content on the hybrid behaviour has been recently addressed [15]. In the 0%–15% range (percentage of rubber by weight in the matrix), K_{IC} showed a maximum constant value above 10% rubber. Every formulation displayed the usual morphology of spherical rubber domains dispersed in a continuous epoxy matrix.

For a particular epoxy–amine–rubber system cured at room temperature, two different types of morphology were observed, depending on the initial rubber content. Our aim was to determine the influence of the morphology type on the mechanical behaviour of toughened epoxies and hybrid materials containing glass beads.

2. Experimental procedure

2.1. Materials

The epoxy resin (DER 332, Dow) was a product based on diglycidylether of bisphenol A (DGEBA), with an

* *Permanent address*: Harbin Institute of Technology, Harbin, People's Republic of China
‡ Author to whom all correspondence should be addressed.

0022–2461

equivalent weight of 174.3 g eq^{-1} as determined by acid titration. The hardener was ethylenediamine (EDA), an analytical grade reagent (Carlo Erba) with an equivalent weight of 15 g eq^{-1}, used in stoichiometric proportions.

The rubber was a carboxyl-terminated acrylonitrile–butadiene random copolymer (CTBN), with a 26% acrylonitrile, a number-average molecular weight of 3200 g mol^{-1} and a polydispersity equal to 2.13 (CTBN 1300 × 13, Goodrich). To ensure a chemical link between rubber particles and the epoxy matrix, CTBN was prereacted with excess DGEBA in the presence of triphenylphosphine as catalyst [16]. This led to an epoxy-terminated acrylonitrile–butadiene (ETBN) random copolymer, available as a solution in excess DGEBA.

Glass beads having a 1.8 g cm^{-3} density and average diameters close to 42 μm were used (fraction with distributions in the 5–50 μm range). They were cleaned with distilled water and isopropyl alcohol, and dried at 100 °C for 24 h. In order to increase the adhesion between particles and matrix, glass beads were coated with a silane adhesion promoter, Z-6020 (*N*-(β-aminoethyl)–γ-aminopropyltrimethoxy silane), supplied by Dow Corning. Glass beads were immersed in a 0.1%–0.5% silane solution in water acidified with acetic acid to a pH in the range 3.5–4. After 24 h, particles were filtered off, dried for another 24 h at 100 °C and sieved to avoid agglomerations.

2.2. Specimen preparation

Glass beads preheated to 100 °C were added, with vigorous stirring, to a DGEBA–ETBN solution, kept at 80 °C. Air bubbles introduced in this procedure were eliminated by degassing under vacuum at 80 °C for 3–4 h. The mixture was cooled to 40–50 °C and the stoichiometric proportion of EDA was added while gently stirring to avoid the introduction of air bubbles (because of the relatively high volatility of EDA (b.p. = 116 °C), applying vacuum after its incorporation was not convenient).

Plates for subsequent mechanical characterization (flexural and fracture tests) were obtained by casting the mixture into a mould consisting of two glass plaques coated with siliconized paper and spaced by a 6 mm diameter rubber cord. Specimens for compression testing were produced by casting the reaction mixture into disposable polypropylene cylindrical moulds.

The mixture was allowed to cure at room temperature for 24 h. During this period phase separation of the rubber from the epoxy matrix took place (judged from the white colour of the resulting materials). Specimens were post-cured at 120 °C for 2 h to drive the epoxy–amine reaction to completion [17].

Henceforth, the glass beads proportion will be denoted as a volume fraction, V_p, whilst the rubber amount will be indicated by the weight percentage of CTBN (the rubbery block of ETBN) in the epoxy–amine–ETBN matrix.

2.3. Mechanical characterization

All mechanical tests were performed at 20 °C and a constant crosshead speed of 0.5 mm min^{-1}, in a Shimadzu Autograph SC-500 universal testing machine. Flexure moduli were determined using sample dimensions recommended by ASTM standards. Uniaxial compression tests were performed on minicylindrical specimens with L/D close to 2 and $D = 5$ mm, deformed between lubricated plates [18]. The nominal strain, e, was determined directly from the crosshead displacement without correcting for the machine softness. The load, P, was converted into true stress, σ, using the initial cross-sectional area, A_0, in the equation

$$\sigma = P(1 - e)/A_0 \quad (1)$$

which is derived assuming constant volume deformation. The yield stress, σ_y, was taken as the maximum of the stress–strain curve. However, for samples containing 15% or more CTBN by weight, a continuous increase of the stress was observed. In these cases, the yield stress was taken as the offset value at 2% strain, i.e. the intersection of the experimental curve and a straight line with a slope equal to the modulus, starting from $e = 0.02$ at $\sigma = 0$.

Fracture tests were performed using single-edge notched specimens (thickness $B = 6$ mm and width $W = 12$ mm), in three-point bending mode (SENB). The span-to-length was $L = 48$ mm. Sharp initial cracks of length a, were obtained by first machining the notch and then generating a natural crack by tapping on a new razor blade placed in the notch of the pre-compressed specimen.

The critical stress intensity factor, K_{IC}, was calculated from

$$K_{IC} = \sigma_c(\pi a)^{1/2} f(a/W) \quad (2)$$

where $\sigma_c = 3P_cL/(2BW^2)$ is the critical stress for crack propagation and $f(a/W)$ is a calibration factor given by

$$f(a/W) = 1.09 - 1.735(a/W) + 8.2(a/W)^2 - 14.18(a/W)^3 + 14.57(a/W)^4 \quad (3)$$

K_{IC} was determined from the slope of a plot of $\sigma_c(\pi a)^{1/2}$ versus $1/f(a/W)$, obtained from at least eight different experimental tests. The length of the initial crack, a, was obtained from the surface of the broken samples using a profile projector (× 10), averaging the results in five points as suggested by ASTM E399 standard.

The strain energy release rate, G_{IC}, was calculated from K_{IC} and E, using the expression for plane strain conditions

$$G_{IC} = (K_{IC}^2/E)(1 - \nu^2) \quad (4)$$

where ν is an average Poisson's ratio of the hybrid material. It was estimated using a rule of mixtures, $\nu = \Sigma V_i \nu_i$, where V_i and ν_i are the volume fraction and the Poisson's ratio of component i (0.35 for epoxy–amine [19], 0.21 for glass [20], and 0.5 for rubber).

2.4. Scanning electron microscopy (SEM)

Fracture surfaces were observed by SEM (Jeol JSM 35 CF), after coating with a fine-gold layer.

3. Results and discussion

3.1. Morphology

Two different types of morphology were generated in the epoxy matrix, depending on the initial rubber amount. Representative pictures are shown in Figs 1–3. All of them correspond to hybrid epoxies containing 25% volume fraction of glass beads but similar results were obtained in the absence of glass particles.

3.1.1. Random dispersion of rubber particles

Up to about 10% CTBN, the morphology consisted of the classic random dispersion of rubber particles. Fig. 1 shows fracture surfaces of materials containing 9% CTBN. Rubber particles with sizes in the range 0.1–0.3 μm are clearly observed at the highest magnification (Fig. 1c). Their volume fraction and average size increased with the CTBN amount in this range. In addition, from Fig. 1b and c, it is observed that glass beads are partially debonded from the matrix.

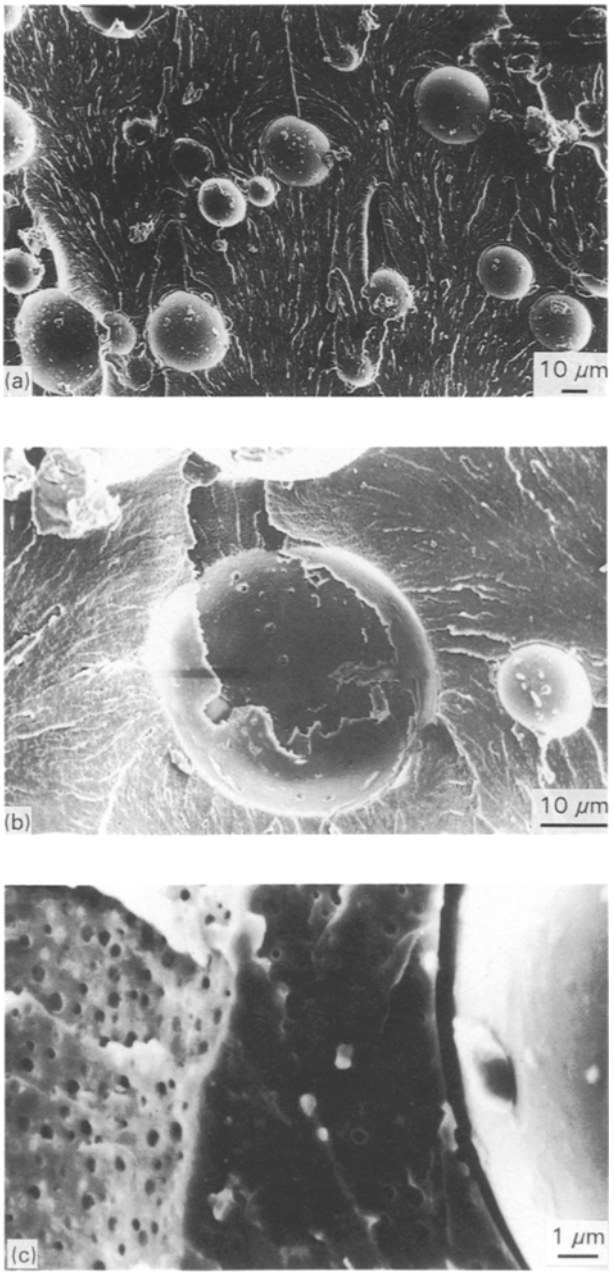

Figure 1 Scanning electron micrographs of hybrids containing 9% CTBN and 25% volume fraction of glass beads.

3.1.2. Irregular domains and co-continuous structures

The morphology becomes completely different when increasing the CTBN amount beyond 10%. Fig. 2 shows the morphology generated for 15% CTBN. Rubbery domains are very much larger in size and have irregular shapes. A secondary phase separation inside dispersed domains may be also observed. At 20% CTBN (Fig. 3) the fracture surface shows a kind of co-continuous structure. This morphology is also characterized by the increase in the debonding of glass beads from the matrix, a fact that decreases the contribution of the crack-pinning mechanism to the fracture toughness [10].

3.1.3. Phase-separation mechanisms

Different morphologies generated in this particular system may be the result of a change in the demixing mechanism with the initial rubber concentration. At low CTBN amounts, phase separation seems to take place by a nucleation–growth mechanism, whereas at high CTBN concentrations, spinodal demixing may be taking place. Factors affecting the phase-separation mechanism have been discussed elsewhere [21]. The

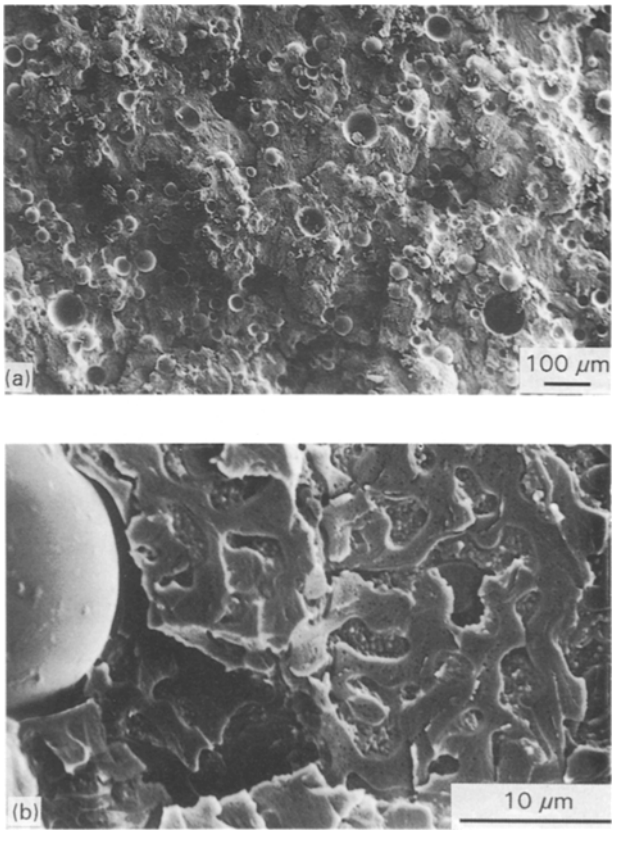

Figure 2 Scanning electron micrographs of hybrids containing 15% CTBN and 25% volume fraction of glass beads.

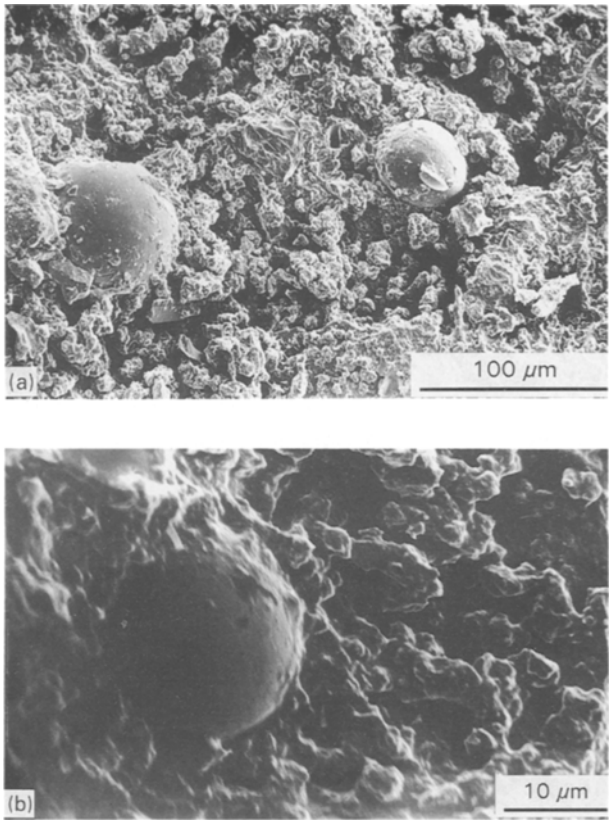

Figure 3 Scanning electron micrographs of hybrids containing 20% CTBN and 25% volume fraction of glass beads.

ratio of polymerization and phase-separation rates in the metastable region and the proximity of the composition to the critical point, are significant factors influencing the nature of the demixing process [21].

In any case, the particular behaviour of the ETBN-modified DGEBA–EDA system, cured at 20 °C, is of interest to assess the influence of the morphology type on mechanical properties of toughened- and particulate-hybrid epoxies.

3.2. Mechanical properties

Fig. 4 shows the flexural modulus, E, of toughened epoxies, as a function of the CTBN amount. E decreases slowly up to 10% CTBN and sharply beyond this value. For 20% CTBN, a 40% reduction in the flexural modulus is attained. The observed behaviour is consistent with the differences in the morphologies generated.

Fig. 5 shows the flexural modulus as a function of the volume fraction of glass beads, for materials containing 0%, 5% and 15% CTBN. A rough fitting of the lower bound of Ishai–Cohen's model [22] is observed for the cases of 0% and 5% CTBN. This model is represented by the following equation

$$\frac{E}{E_m} = \frac{V_p}{\left(\frac{m}{m-1} - V_p^{1/3}\right)} \quad (5)$$

where E_m is the elastic modulus of the toughened matrix (obtained from Fig. 4 for the various CTBN amounts), and $m = E_p/E_m$, is the ratio between the elastic modulus of the glass beads and that of the matrix. E_p was taken as 73.1 GPa [3, 6].

As E increases with V_p and decreases with percentage of CTBN, a desired value may be attained by a convenient combination of rubbery and rigid phases.

The uniaxial compression yield stress as a function of V_p and percentage of CTBN is shown in Figs 6 and 7. Rubber particles possess a lower shear modulus than the epoxy matrix and, consequently, they are

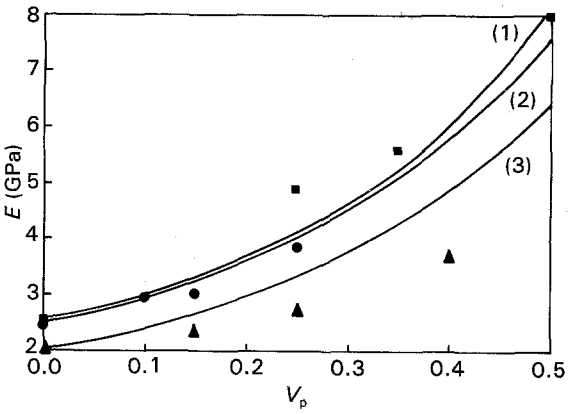

Figure 5 Flexural modulus as a function of the volume fraction of glass beads for materials containing (■) 0, (●) 5 and (▲) 15% CTBN. (——) Predicted values from the Ishai–Cohen model [22], for the case of uniform displacement at the particle–matrix interface: (1) 0%, (2) 5%, (3) 15% CTBN.

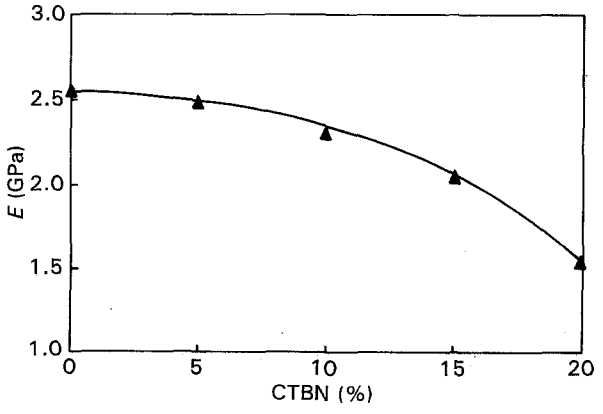

Figure 4 Flexural modulus as a function of the rubber content for toughened epoxies devoid of glass beads.

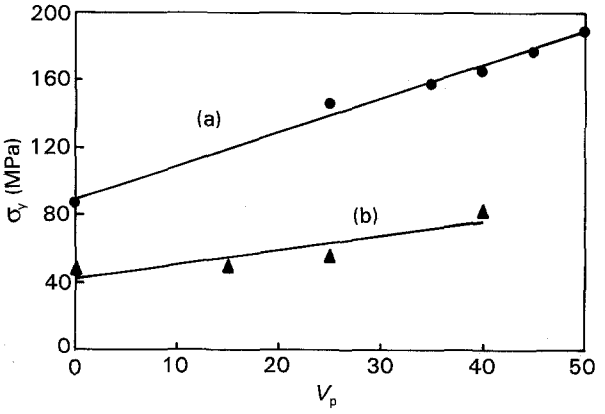

Figure 6 Yield stress as a function of the volume fraction of glass beads, (a) without CTBN, (b) with 15% CTBN.

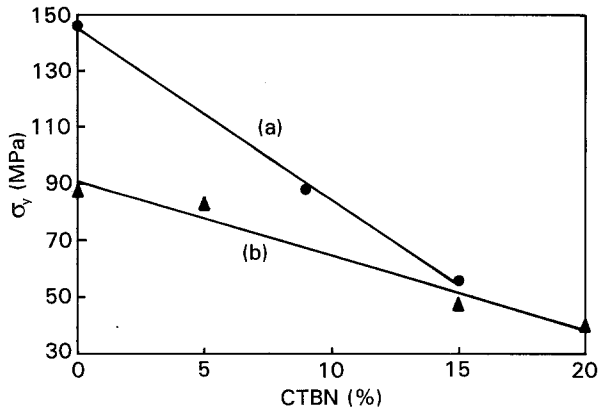

Figure 7 Yield stress as a function of the rubber content. (a) 25% by volume of glass beads, (b) without glass beads.

unable to support a significant share of the stress. This is the origin of the yield-stress reduction produced by the CTBN incorporation.

Hybrids containing 15% CTBN exhibit very low values of σ_y, independently of the presence of glass beads. Clearly, at this CTBN level, the overall behaviour is dominated by the matrix properties. On the other hand, a high increase in σ_y is produced by the addition of glass beads to epoxy–amine formulations devoid of rubber.

Fracture tests revealed a stick–slip mode of fracture when CTBN was incorporated to the formulation. In this case, the initiation value of K_{IC} was calculated. Fig. 8 shows K_{IC} as a function of the CTBN amount for hybrids containing 25% by volume of glass beads (curve a) and for toughened epoxies devoid of glass (curve b). An increase in K_{IC} with the CTBN amount is observed in the 0%–10% range, consistently with the decrease in σ_y. This enhances the crack-tip blunting and increases the critical stress necessary to propagate the crack [23]. Localized plastic shear-yielding and cavitation of rubber particles (Fig. 1c) occur in the vicinity of the propagating crack tip. Plastic deformation results in a partial debonding of glass particles from the epoxy matrix (see Fig. 1 and [9]).

The change in the morphology generated with CTBN additions higher than 10%, leads to an abrupt decrease in K_{IC}. This behaviour may be ascribed to the mechanical weakness of these morphologies, characterized by very low σ_y values. Cracks need relatively low critical stresses to propagate through these structures.

The presence of glass beads incorporates the crack-pinning mechanism causing an increase in K_{IC} (Fig. 9). Similar behaviour was reported by other authors [4, 5, 15]. The addition of 15% CTBN has a very small influence on K_{IC}, independently of the rigid filler fraction. Therefore, morphologies generated at high CTBN amounts lead to poor mechanical properties, a fact that cannot be modified through the addition of glass beads.

The variation in the strain energy release rate, G_{IC}, as a function of the CTBN amount, is shown in Fig. 10. A four-fold increase in G_{IC} is observed for the hybrid containing 9% CTBN and 25% volume fraction of glass beads. Whilst the addition of 25% by volume of glass beads to the pure epoxy–amine matrix does not practically modify the G_{IC} value, the additional incorporation of 9% CTBN promotes a significant increase in G_{IC}. This synergetic effect is the basis of the considerable increase in toughness exhibited by hybrid–particulate composites.

4. Conclusion

A particulate rubber-toughened epoxy formulation exhibiting different morphologies as a function of the rubber content was developed. Up to 10% rubber, the

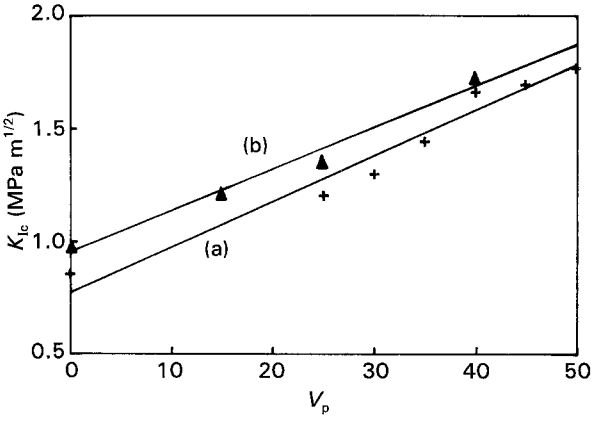

Figure 9 Critical stress intensity factor as a function of the volume fraction of glass beads: (a) without CTBN, (b) with 15% CTBN.

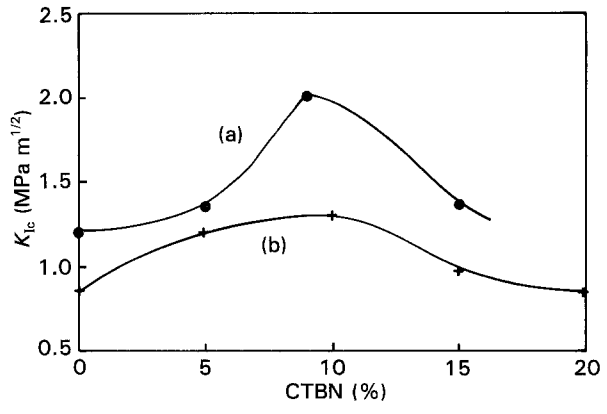

Figure 8 Critical stress intensity factor as a function of the rubber content: (a) 25% by volume of glass beads, (b) without glass beads.

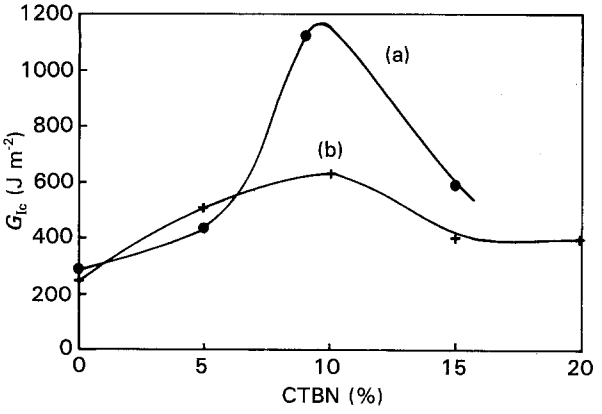

Figure 10 Strain energy release rate as a function of the rubber content: (a) 25% by volume of glass beads, (b) without glass beads.

morphology consisted of the classic random dispersion of spherical domains rich in rubber. At 15% rubber, large and irregular domains were observed. At 20% rubber, a co-continuous structure was generated. This was ascribed to a change in the phase-separation mechanism from nucleation–growth to spinodal demixing.

Mechanical properties of the toughened epoxies and hybrid–particulate materials containing glass beads were analysed. The best mechanical properties were obtained for systems exhibiting the random dispersion of spherical domains, in particular for the largest amount of rubber producing this morphology (about 10% rubber by weight for the particular formulation investigated). Morphologies consisting of large and irregular domains or co-continuous structures, exhibited low values of the flexural modulus, yield stress and fracture toughness.

Hybrid–particulate materials containing about 10% by weight of rubber and 25% by volume of glass-beads showed a considerable increase in fracture toughness, arising from a synergetic effect of the different micromechanisms of crack propagation.

References

1. D. VERCHERE, J. P. PASCAULT, H. SAUTEREAU, S. M. MOSCHIAR, C. C. RICCARDI and R. J. J. WILLIAMS, *J. Appl. Polym. Sci.* **43** (1991) 293.
2. K. C. RADFORD, *J. Mater. Sci.* **6** (1971) 1286.
3. R. J. YOUNG and P. W. R. BEAUMONT, *ibid.* **12** (1977) 684.
4. A. C. MOLONEY, H. H. KAUSCH and H. R. STIEGER, *ibid.* **18** (1983) 208.
5. *Idem, ibid.* **19** (1984) 1125.
6. J. SPANOUDAKIS and R. J. YOUNG, *ibid.* **19** (1984) 473.
7. *Idem, ibid.* **19** (1984) 487.
8. D. L. MAXWELL, R. J. YOUNG and A. J. KINLOCH, *J. Mater. Sci. Lett.* **3** (1984) 9.
9. A. J. KINLOCH, D. L. MAXWELL and R. J. YOUNG, *ibid.* **4** (1985) 1276.
10. *Idem, J. Mater. Sci.* **20** (1985) 4169.
11. R. J. YOUNG, D. L. MAXWELL and A. J. KINLOCH, *ibid.* **21** (1986) 380.
12. A. C. MOLONEY, H. H. KAUSCH, T. KAISER and H. R. BEER, *ibid.* **22** (1987) 381.
13. A. C. ROULIN-MOLONEY, W. J. CANTWELL and H. H. KAUSCH, *Polym. Compos.* **8** (1987) 314.
14. S. BANDYOPADHYAY, V. M. SILVA, I. M. LOW and Y. W. MAI, *Plast. Rubb. Proc. Appl.* **10** (1988) 193.
15. A. MAAZOUZ, H. SAUTEREAU and J. F. GERARD, *J. Appl. Polym. Sci.* **50** (1993) 615.
16. D. VERCHERE, H. SAUTEREAU, J. P. PASCAULT, S. M. MOSCHIAR, C. C. RICCARDI, R. J. J. WILLIAMS, *Polymer* **30** (1989) 107.
17. C. C. RICCARDI, H. E. ADABBO and R. J. J. WILLIAMS, *J. Appl. Polym. Sci.* **29** (1984) 2481.
18. S. YAMINI and R. J. YOUNG, *J. Mater. Sci.* **15** (1980) 1814.
19. *Idem, ibid.* **14** (1979) 1609.
20. N. AMDOUNI, H. SAUTEREAU, J. F. GERARD, F. FERNAGUT, G. COULON and J. M. LEFEBVRE, *ibid.* **25** (1990) 1435.
21. D. VERCHERE, H. SAUTEREAU, J. P. PASCAULT, S. M. MOSCHIAR, C. C. RICCARDI and R. J. J. WILLIAMS, in "Toughened Plastics I, Science and Engineering", Advances in Chemistry Series, Vol. 233, edited by C. K. Riew and A. J. Kinloch (American Chemical Society, Washington DC, 1993) p. 335.
22. O. ISHAI and L. J. COHEN, *Int. J. Mech. Sci.* **9** (1967) 539.
23. A. J. KINLOCH and J. G. WILLIAMS, *J. Mater. Sci.* **15** (1980) 987.

Received 20 November 1992
and accepted 19 October 1993